The Long Neglected Cycloidal Mass Analyzer

Elettra Piacentino[¶], Rafael Bento Serpa[¶], Kathleen Horvath[¶], Raul Vyas[¶], Tanouir Aloui[¶], Charles B. Parker[¶], James B. Carlson[‡], Justin Keogh[^], Roger P. Sperline[^], Luisa Sartorelli^{¶a}, Brian R. Stoner[¶], Michael E. Gehm[¶], Jeffrey T. Glass[¶], M. Bonner Denton[^], Jason J. Amsden[¶],*

Author Affiliations:

[¶]Department of Electrical and Computer Engineering, Duke University, Durham, NC, USA 27708

[‡] Engineering and Applied Physics Division, RTI International, Research Triangle Park, NC USA 27709

^Department of Chemistry and Biochemistry, University of Arizona, Tucson, AZ USA 85721

^aDepartamento de Física, Universidade Federal de Santa Catarina, Campus Universitário Trindade, 88040-000 Florianópolis, SC BRAZIL

*Corresponding Author:

Jason J. Amsden

Department of Electrical and Computer Engineering

Duke University

Durham, NC 27708

919-348-1574

jason.amsden@duke.edu

Abstract

In 1938, Walker Bleakney and John A. Hipple first described the cycloidal mass analyzer

as the only mass analyzer configuration capable of "perfect" ion focusing. Why has their

geometry been largely neglected for many years and how might it earn a respectable

place in the world of modern chemical analysis? This perspective explores the properties

of the cycloidal mass analyzer and identifies the lack of suitable ion array detectors as a

significant reason why cycloidal mass analyzers are not widely used. The recent

development of capacitive transimpedance amplifier array detectors can enable several

techniques using cycloidal mass analyzers including spatially coded apertures and single

particle mass analysis with a "virtual-slit", helping the cycloidal mass analyzer earn a

respectable place in chemical analysis.

Keywords: cycloid, mass analyzer, sector, array detector

3

1 Introduction

In 1938, Walker Bleakney and John A. Hipple Jr. described the cycloidal mass analyzer, and pointed out that the cycloidal mass analyzer configuration was the only perfect-focusing mass analyzer described at that date. The cycloidal mass analyzer utilizes homogenous, perpendicularly oriented magnetic and electric fields, to separate ions based on their mass-to-charge ratio (m/q). Ions in a cycloidal mass analyzer travel along cycloidal trajectories in a plane perpendicular to the magnetic field. Cycloidal trajectories refer to the path of a point rigidly attached inside, outside, or on a circle rolling on a fixed line. The movement of ions in a cycloidal mass analyzer is summarized by Equation 1 where the focal distance a_i , referred to as the pitch, is the distance along the focal plane from the ion source exit slit to the location of the ion following one full revolution of the circle describing the cycloid, m_i represents the i^{th} ion with charge q, E is in the uniform electric field, and B is the uniform magnetic field.

$$a_i = \frac{m_i}{q} \frac{2\pi E}{B^2}$$

The pitch or focus position is independent of the initial velocity vector of the ions. This is a key advantage of the cycloidal mass analyzer over other double focusing sector mass analyzers that only correct for small initial velocity distributions. Additionally, cycloidal mass analyzers offer a focal plane. When a suitable array detector is placed at the focal plane of a cycloidal mass analyzer, it allows simultaneous monitoring of a wide mass range of ions with a 100% duty cycle – all ions at different m/q are measured all the time. These capabilities are advantageous for analysis involving high precision isotope ratios, small sample sizes, or transient events. Furthermore, cycloidal mass analyzers have a

small footprint due to the overlapping electric and magnetic sectors leading to a small ion flight path and reduced vacuum requirements.

Despite the many advantages of cycloidal mass analyzers, since their introduction in 1938, there have been relatively few publications related to their use. The authors feel that it is probable that many readers of the Analytical Chemistry journal are not aware of the unique characteristics offered by the cycloidal geometry. In fact, in the Analytical Chemistry journal over the past 30 years, we have only been able to find brief mentions of the cycloidal geometry in a few review articles.³⁻⁵ While probably not totally exhaustive, searching as widely as possible throughout the literature, we have only located approximately seventy manuscripts published about the cycloidal mass analyzer since it was first introduced in 1938 (Blase et al.⁶ and Amsden et al.⁷ provide a summary of most of the available cycloidal mass analyzer literature). The relative lack of publications utilizing the cycloidal mass analyzer is due in part to the requirement of a suitable ion array detector to fully take advantage of the unique focusing properties of the cycloidal mass analyzer. This perspective reviews the focusing properties of the cycloidal mass analyzer; discusses the detector requirements for a cycloidal mass analyzer that lead to the relative neglect of cycloidal mass analyzers over the years; discusses how the recently developed capacitive transimpedance amplifier (CTIA) array detector meets these requirements; and finally discusses some unique current and future applications of the cycloidal mass analyzer with the CTIA detector that might earn it a respectable place in the world of modern chemical analysis.

2 Cycloidal mass analyzer equations of motion

A cycloidal mass analyzer employs the motion of ions in perpendicularly oriented homogeneous electric and magnetic fields. Here we will review the solutions for the equations of motion for ions in a cycloidal mass analyzer to show how the crossed electric and magnetic fields produce the unique focusing properties of the cycloidal mass analyzer.

To start, we will assume a uniform electric field E oriented in the -y direction, a uniform magnetic field E along the -z direction, and ions of mass E (where E = 1, 2, ... total number of ions) and charge E (see Figure 1). Using the Lorentz force law (Equation 2) yields the equations of motion for the x-, y-, and z-coordinates (Equations 3-5) of the ions, where the double dot denotes the second derivative with respect to time and the single dot denotes the first derivative with respect to time.

$\vec{F} = m_i \vec{a} = q \vec{E} + q \vec{v} \times \vec{B}$	2
$\ddot{x}_i = -\frac{qB}{m_i}\dot{y}_i$	3
$\ddot{y}_i = -\frac{qE}{m_i} + \frac{qB}{m_i} \dot{x}_i$	4
$\ddot{z_i} = 0$	5

Equations 6-8 are the solutions to the equations of motion using the initial conditions in Table 1. Equations 6-8 are parametric equations that describe the cycloidal trajectories

for ions of mass m_i and charge q in perpendicularly oriented electric and magnetic fields, where $\Omega = \frac{qB}{m_i}$.

Table 1. Initial conditions for a cycloidal mass analyzer

Initial velocities	$\dot{x}_i(0) = v_{ix0}, \ \dot{y}_i(0) = v_{iy0}, \ \dot{z}_i(0) = v_{iz0}$
Initial positions	$x_i(0) = x_{oi}, \ y_i(0) = y_{oi}, \ z_i(0) = z_{oi}$

$x_i(t) = \frac{E}{B}t + \frac{v_{iy0}}{\Omega}\cos(\Omega t) + \frac{1}{\Omega}\left(v_{x0} - \frac{E}{B}\right)\sin(\Omega t) - \frac{v_{iy0}}{\Omega} + x_{oi}$	6
$y_i(t) = \frac{1}{\Omega} \left(\frac{E}{B} - v_{ix0} \right) \cos(\Omega t) + \frac{v_{iy0}}{\Omega} \sin(\Omega t) - \frac{E}{B\Omega} + \frac{v_{ix0}}{\Omega} + y_{oi}$	7
$z_i(t) = v_{iz0}t + z_{oi}$	8

Note that at time $t_i = \frac{2\pi m_i}{qB}$, $y_i(t_i) = y_{oi}$, and $x_i(t_i) = a_i = \frac{m_i}{q} \frac{2\pi E}{B^2} + x_{oi}$. The y-coordinate of the ion returns to the original position while the x-coordinate is shifted by the pitch a_i of the cycloid for each m_i/q (Equation 1). Note that $x_i(t_i) = a_i = \frac{m_i}{q} \frac{2\pi E}{B^2} + x_{oi}$ does not depend on the initial velocity vector of the ion. The lack of dependence of the pitch on the initial velocity is the perfect focusing property of the cycloidal mass analyzer. In addition, Equation 1 shows that the cycloidal mass analyzer offers a focal plane with which an appropriate array detector can simultaneously detect a wide range of mass to charge ratios.

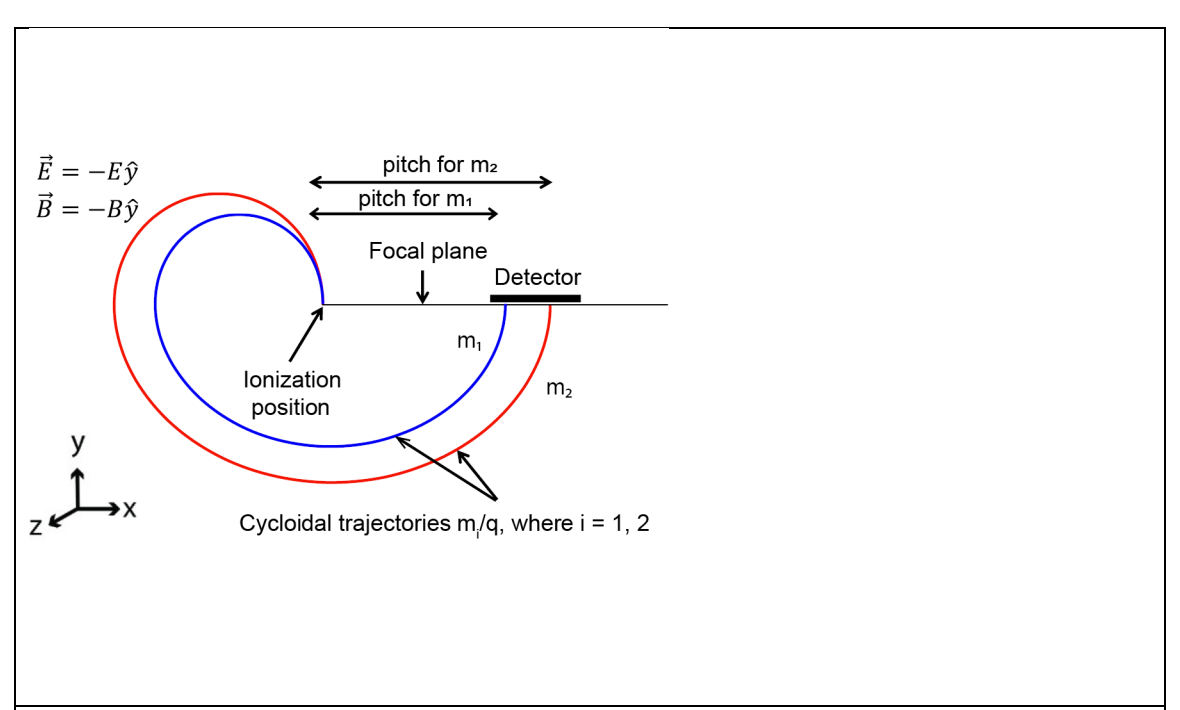


Figure 1. Cycloidal trajectories for two ions m_1/q and m_2/q traveling in homogeneous perpendicularly oriented electric and magnetic fields.

Note that the cycloidal mass analyzer does not have any focusing along the z-direction (Equation 8) and ions with z-velocity components are dispersed along a line parallel to the z-axis passing through the x-coordinate for the pitch. However, in most ion sources, such as a Nier type electron ionization source, source, ions are not accelerated in the z-direction; therefore the initial velocity in the z-direction is just the thermal velocity which does not lead to significant spread in the z-direction. For example, N_2 has a mean thermal velocity of 480 m/s at room temperature based on the Maxwell-Boltzmann velocity distribution. A N_2 + ion in a cycloidal mass analyzer with a 0.5 T magnetic field would take 3.6 μ s to travel a cycloidal trajectory ($t = \frac{2\pi m}{q_B}$), and in that time, travel an average of only 1.7 mm in the z-direction due to the thermal velocity. Therefore, as long as the detector pixels are longer than the spread induced by the thermal velocity, no significant loss in ions will occur.

3 Detector requirements for a cycloidal mass analyzer

As mentioned above, an ion array detector is required to take full advantage of the unique perfect focusing properties of the cycloidal mass analyzer. Most previously demonstrated cycloidal instruments used a single detector element and therefore did not have significant advantages over other serial instruments, such as quadrupoles and ion traps. An ion array detector must have two properties to function in a cycloidal mass analyzer. First, the detector must be capable of operating inside the magnetic field. Second, since the size of the cycloidal trajectories depends on the ion energy, it is preferable to operate the cycloidal mass analyzer at relatively low ion energies (5-50 eV), so the detector should be able to efficiently detect low energy ions.

The most common ion detectors today fall into two categories - Faraday cups and electron multipliers. Faraday cups have high dynamic range and have been used in array configurations. However, they have relatively low sensitivity. Electron multipliers have much higher sensitivity and can also be used in an array format such as a multichannel plate detector. However, electron multipliers suffer from poor performance when operated in magnetic fields as ejected electrons will follow spiral, cyclotron paths in the magnetic field and not reach the next dynode. Since the cycloidal mass analyzer focal plane lies in the magnetic field, electron multiplier detectors are a poor choice for use with cycloidal mass analyzers. In 1974, Adams and Smith recognized the utility of array detectors when coupled with cycloidal mass analyzers. However, they employed an electron multiplier type array detector and their prototype suffered from poor performance. Faraday cups and have been used in array and have been used in array and have been used in array array detectors will follow spiral.

at low ion energies. In general, electron multiplier type detectors are inefficient at low incident ion energies. ¹⁴ Therefore, the lack of a suitable detector technology is a significant reason for the limited use of cycloidal mass analyzers despite their many advantages.

4 The solution: CTIA array detectors

CTIA ion detectors provide a solution to the detector problem for cycloidal mass analyzers. CTIA ion detectors are similar to Faraday cups. However, in the CTIA amplifier, a small capacitor is used instead of the resistor used in the Faraday cup amplifier circuit. The CTIA detector enables direct charge detection and operation with low ion energies, even in a magnetic field. CTIA detectors have been demonstrated in a variety of array configurations including a version fabricated using standard complementary metal oxide semiconductor (CMOS) techniques with 1704 12.5 μ m wide by 3 mm tall pixels that are arranged in such a way as to provide a 100% fill factor. The pixels are fabricated on a CMOS die along with the amplifiers, and each pixel has multiple gain levels that are individually programmable. CTIA detector arrays have been demonstrated with a sensitivity of 15 μ V/e- at high gain and a dynamic range of 10^{11} using the multiple gain levels, approaching the sensitivity of an electron multiplier and exceeding the dynamic range of a Faraday cup. $^{9,15-22}$

5 Current and future applications of cycloidal mass analyzers with array detectors

The availability of high performance CTIA array detectors that can detect ions with low energies and operate in magnetic fields should help earn the cycloidal mass analyzer a

prominent place in the world of modern chemical analysis commensurate with its unique perfect focusing properties. In the following two subsections we review the recent demonstration of a proof-of-concept instrument incorporating a cycloidal mass analyzer with a CTIA array detector and spatially coded apertures, and introduce a potential new application of cycloidal mass analyzers coupled with array detectors enabling "virtual-slit" focusing to improve the sensitivity of portable single particle mass analyzers.

5.1 Computational sensing and spatially coded apertures

Spatially coded apertures are a technique used in optical spectroscopy to increase the throughput of a spectrometer without sacrificing resolution.²³ An analogous method was proposed in sector mass spectrometry in 1970.²⁴ However, the first demonstration was not until 2014, when Chen et al.²⁵ and Russell et al.²⁶ used spatially coded apertures with a 90-degree magnetic sector mass spectrometer and a multichannel plate and phosphor screen detector.²⁷ Although coded apertures worked with the 90-degree sector, the limited mass range and low resolution resulting from dispersion in the ion source limited the utility of the 90-degree sector with spatially coded apertures.

In 2018, Amsden *et al.* demonstrated spatially coded apertures in a miniature cycloidal mass analyzer incorporating a 1704 channel CTIA array detector.⁷ Figure 2A and B show the raw data for a slit and coded aperture respectively, while Figure 2C shows the coded spectrum from Figure 2B after reconstruction. The cycloidal mass analyzer projects an image of the slit pattern on the CTIA array detector for each m/q. The image is not an exact match due to field non-uniformities and misalignment of the detector with the

cycloidal mass analyzer focal plane. However, upon reconstruction, a >10-fold increase in signal is observed compared to the slit mass spectrum, with no loss in resolution. In fact, the resolution of the reconstructed spectrum is improved compared to the slit mass spectrum due to the deconvolution of the peak shape from the data. Due to the perfect focusing properties of the cycloidal mass analyzer, the reconstruction procedure for the coded spectra involved a simple deconvolution of the aperture image from the data, replacing the much more complex reconstruction process used in the 90-degree sector. This example of spatially coded apertures increasing throughput without sacrificing resolution using a simple deconvolution for the reconstruction process shows the power of cycloidal mass analyzers coupled with array detectors not previously realized due to the absence of a detector technology capable of operating in a magnetic field.

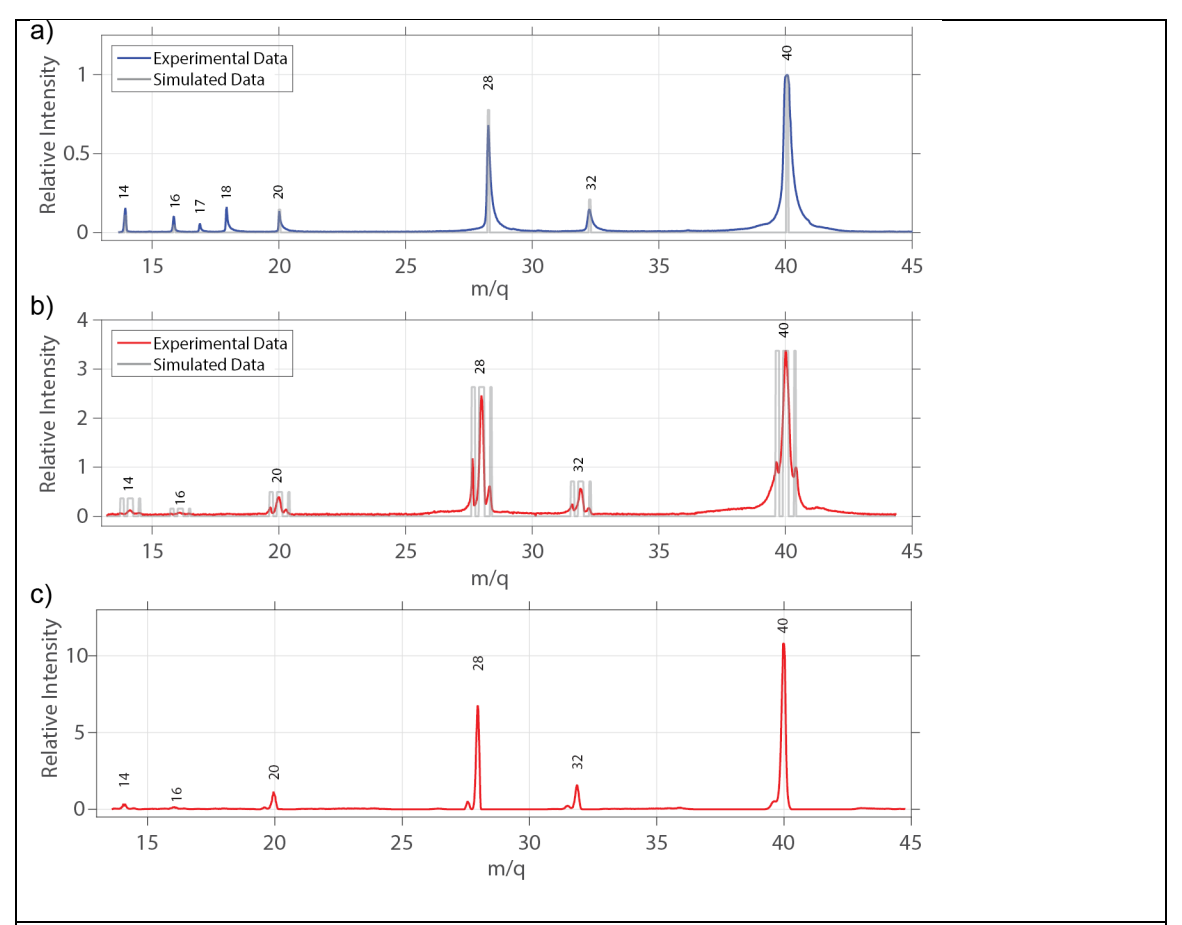


Figure 2. Slit and coded aperture spectra from a cycloidal mass analyzer incorporating a CTIA array detector. (A) Mass spectrum of a mix of 50% pure argon and 50% dry air using a 50 µm slit. (B) Coded mass spectrum of a mix of 50% pure argon and 50% dry air using a coded aperture with three slits: 100 μm, 150 μm, and 50 um wide, separated by 100 µm and 150 µm, respectively. In both A and B, the colored traces represents the experimental data and the grey histogram represents an ideal system based on the data from the NIST Chemistry WebBook.²⁸ In addition, A, B, and C are normalized such that the relative intensity of the smallest slit is 1. (C) Reconstructed data from Figure 2B, showing an order of magnitude increase in signal with no loss in resolution. Adapted with permission from Amsden, J. J.; Herr, P. J.; Landry, D. M. W.; Kim, W.; Vyas, R.; Parker, C. B.; Kirley, M. P.; Keil, A. D.; Gilchrist, K. H.; Radauscher, E. J.; Hall, S. D.; Carlson, J. B.; Baldasaro, N.; Stokes, D.; Di Dona, S. T.; Russell, Z. E.; Grego, S.; Edwards, S. J.; Sperline, R. P.; Denton, M. B.; Stoner, B. R.; Gehm, M. E.; Glass, J. T., Proof of Concept Coded Aperture Miniature Mass Spectrometer Using a Cycloidal Sector Mass Analyzer, a Carbon Nanotube (CNT) Field Emission Electron Ionization Source, and an Array Detector. J Am Soc Mass Spectrom 2018, 29 (2), 360-372. Copyright 2018 American Chemical Society.

5.2 Virtual-slit single particle analyzers

The cycloidal mas analyzer coupled with an array detector could enable a portable high sensitivity mass analyzer for single particle analysis with laser ionization. A typical single particle mass spectrometer (SPMS) is comprised of four parts including an inlet, ion source, mass analyzer, and detector. The inlet system for a SPMS usually includes an aerosol particle inlet and particle sizer that produces a stream of particles, measures their size, and enables synchronizing an ionizing laser pulse with the arrival of a particle in the ion source. Ionization is typically accomplished by pulsed laser ionization using a UV harmonic of a Nd:YAG laser or an excimer laser. Mass analysis is most often accomplished via a time-of-flight (TOF) mass analyzer and detection is usually accomplished using multichannel plate (MCP) amplifiers. ^{29,30} Developing a portable single particle mass analyzer involves a number of challenges including collecting ions with the wide energy and angular distributions generated by the laser ionization and overcoming the throughput vs. resolution tradeoff in spectrometer miniaturization.

When ionizing a particle with laser ionization, ions are created with velocities in all directions and with a wide energy spread (typically 0-60 eV with the peak around 20-30 eV). Figure 3A and B show the difficulty in collecting ions with wide angular and energy spreads such as that created by laser ionization. In Figure 3A where no focusing is used, very few of the ions generated by laser ionization are directed towards the entrance slit of the mass analyzer, resulting in poor sensitivity. In Figure 3B, to increase analysis efficiency and sensitivity, a focusing electrode is used to direct ions moving away from the slit back towards the slit. However, this leads to an increase in ion energy and energy

dispersion and many ions still do not reach the mass analyzer. Double focusing sector instruments^{32, 33} and TOF instruments employing a reflectron^{34, 35} can compensate for some energy and angular dispersion in the ion beam. However, a large double focusing or TOF instrument is required to adequately compensate for the dispersion in order to achieve the necessary sensitivity and resolution.

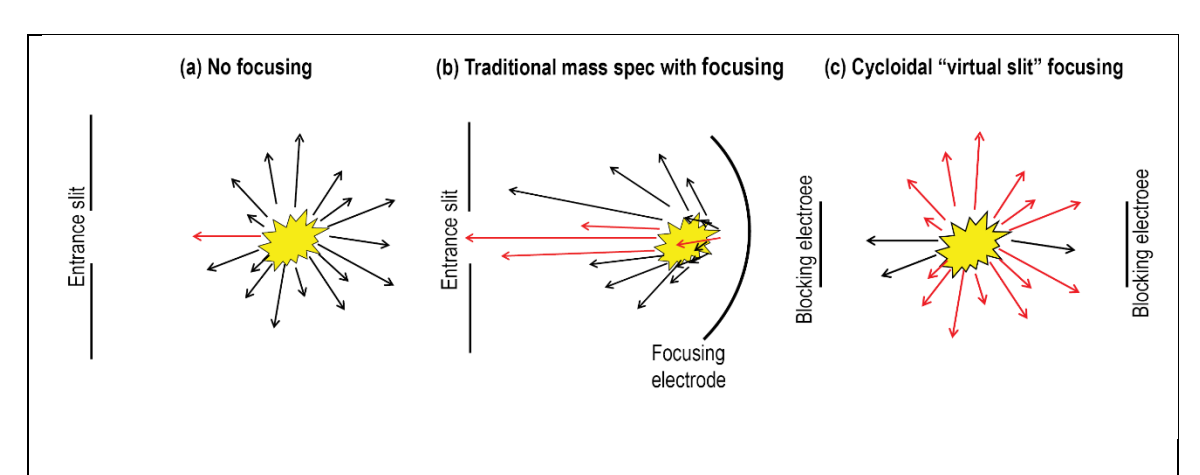


Figure 3. Comparison of different focusing options for laser ionization, leading to dramatically different ion utilization efficiencies. In the three cases, the arrows represent ion trajectories and their lengths represent the ion energy. Red arrows enter the mass analyzer through the slit and are analyzed. Black arrows are lost and not analyzed. (A) No focusing: laser ionization produces ions in all directions with a wide energy spread. In this case, only the ion with the red arrow enters the mass analyzer entrance slit. All other ions are lost and not analyzed. (B) Conventional focusing: In conventional mass analyzer a focusing electrode is added to redirect ions moving away from the mass analyzer towards the entrance slit. More ions enter the mass analyzer at the expense of increased energy dispersion. This requires a large instrument to compensate for the dispersion and to achieve sufficient resolution. (C) Cycloidal focusing: here, no slits are needed and the particle is ionized directly inside the mass analyzer and the size of the particle to be ionized acts as a virtual-slit. The vast majority of ions are analyzed due to the unique focusing properties of the cycloidal mass analyzer. In practice, a small number of ions with initial velocities parallel to the focal plane will hit the detector before undergoing a full cycloidal revolution, so two blocking electrodes are placed on either side of the ionization position to block these ions

A second issue with portable SPMS instruments is that they suffer from a throughput vs. resolution tradeoff.²⁷ To maintain high resolution when shrinking a sector-based mass

spectrometer instrument, the entrance slit must also shrink leading to lower throughput and sensitivity. With a TOF instrument, reducing the size of the instrument leads to decreased resolution due to ions of different mass to charge ratios reaching the detector with smaller time differences.

The perfect focusing properties of the cycloidal mass analyzer coupled with the CTIA array detector provides solutions to the challenges of collecting ions with wide energy and angular dispersions generated by laser ionization and overcoming the throughput vs resolution tradeoff discussed above for single particle mass spectrometry.

First, as the pitch a (see Equation 1) of the cycloidal analyzer does not depend on the initial energy or direction of the ion leaving the ion source, it can collect ions emitted at all energies and angles. Figure 4A-C shows trajectories using m/q = 300 u ions, illustrating the ability of a cycloidal mass analyzer to focus ions with wide energy dispersion (Figure 4A), large angular dispersion (Figure 4B), and a combination of both energy and angular dispersions (Figure 4C). In practice, the size of the cycloidal path traced by the ion is determined by the ion energy (Figure 4A). In addition, a double-sided detector would be required to collect ions with initial velocities in the +y or -y directions as ions with initial velocity components in the +y direction will reach one side of the detector while ions with initial velocity components in the -y direction will hit the other side. Currently a double-sided ion array detector does not exist. However, it would be similar in construction to backside-thinned CCDs that have been in use since the 1980s.³⁶

Figure 5 shows a schematic and photograph of a single-sided CTIA array detector along with a conceptual schematic for a double-sided CTIA array detector.

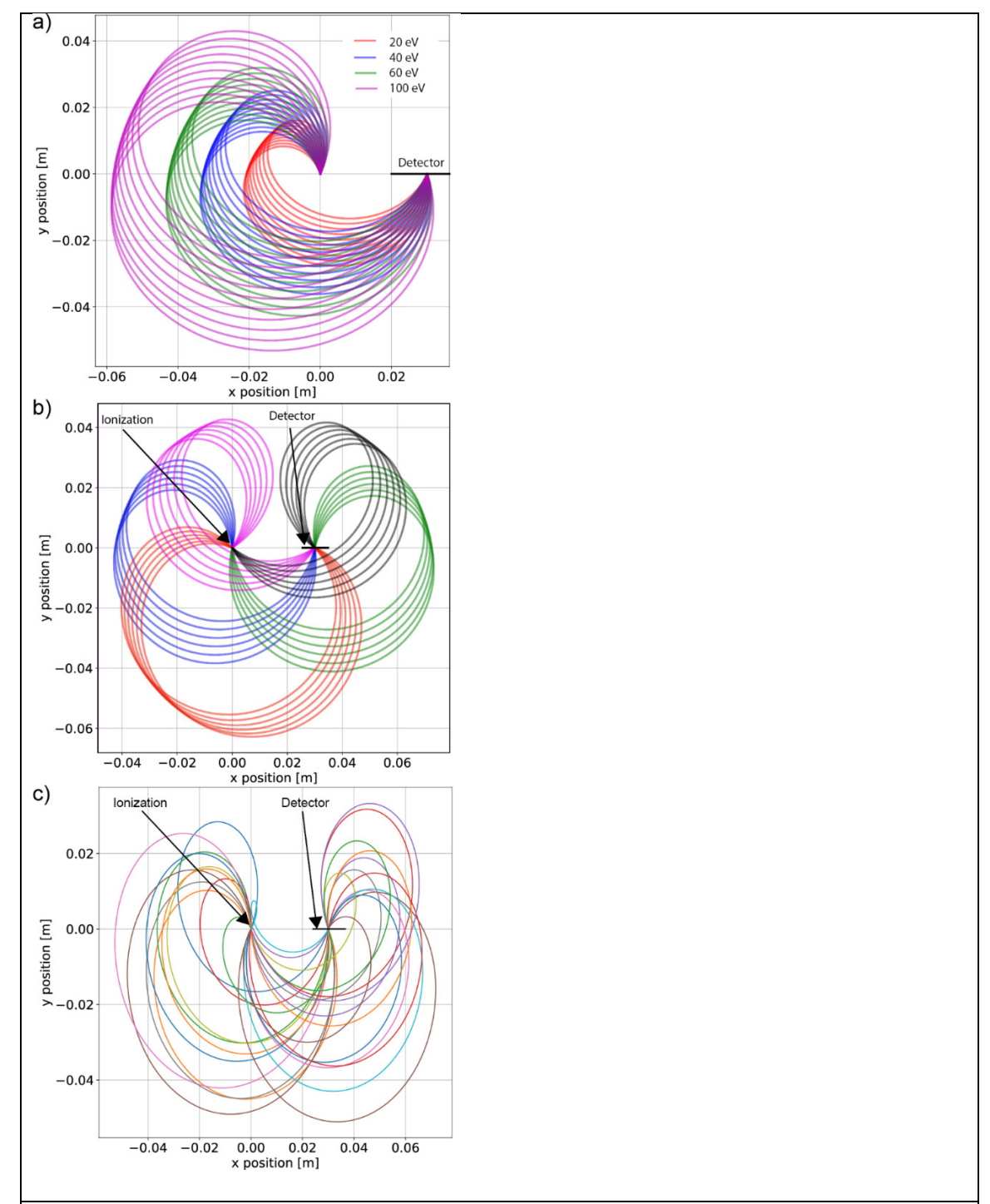


Figure 4. (A) Cycloidal trajectories for m/q = 300 ions with energies of 20, 40, 60, and 100 eV for a 45° spread of initial angles measured from the y-axis showing focusing of a 5-fold range of energies. (B) Cycloidal trajectories for a m/q = 300 ions and constant energy of 40 eV and 5 groups of ions with a range of different angles from 0-360° all

focused at the same spot on a double-sided detector. In these calculations, the magnetic field is 0.7 T and electric field is 7.52 V/cm. (C) Cyloidal trajectories for 25 m/q = 300 ions with random energies and directions. The ion source is at position (0,0), and the detector is a 10 mm wide strip extending along the x-axis from x = 25 mm to x = 35 mm. m/q = 300 ions with an energy distribution of 40 ± 20 eV emanate from a 10 μ m sphere in all directions. Ions with initial angles of > $\pm45^{\circ}$ measured from the x-axis are blocked as ions exiting at these angles may hit the detector before completing a full revolution of the cycloidal path.

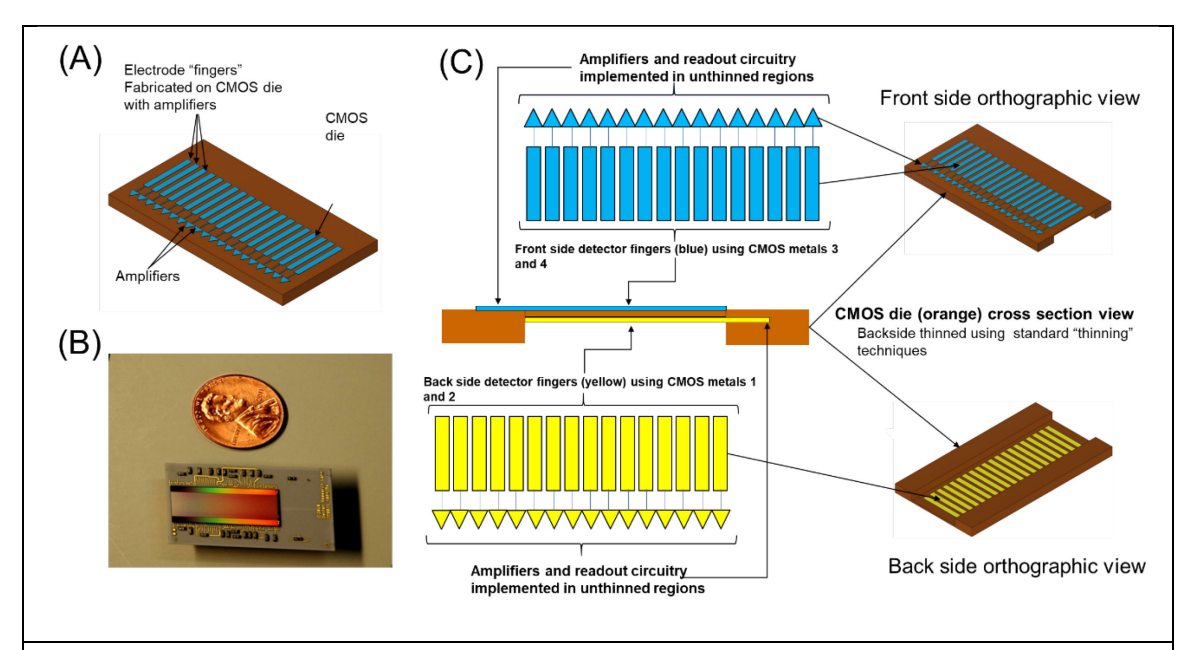


Figure 5. (A) Single-sided CMOS CTIA detector configuration employing monolithic collection electrodes. The implementation incorporates amplifiers which are individually gain programmable, as well as all the readout circuitry on the CMOS die. (B) Photograph of a single-sided CMOS CTIA array detector. (C) Proposed double-sided CTIA array detector. Similar to the single-sided configuration already demonstrated, a double-sided CTIA array detector would be fabricated with standard CMOS processing. The detector pixels or "fingers" would be fabricated on the CMOS die along with the individually programmable gain amplifiers and redout circuitry. The front side configuration would use metal layers 1 and 2 of the CMOS process for the detector pixels while the back side configuration would use metal layers 3 and 4. After fabrication, the back side would be thinned to reveal metal layers 3 and 4 while the amplifiers and readout circuitry would remain in the unthinned sections.

Second, the focusing properties enable using the particle as a "virtual-slit", removing the need for an actual physical slit or ion source. For a cycloidal mass analyzer, the resolving

power, $\frac{m}{\Delta m}$ where m is the mass of the selected ion and Δm is the width of the mass peak

is equivalent to Δa , where a is the pitch of the selected m/q (see Equation 1) and Δa is the width of the peak at the array detector.^{1, 13} For the perfect focusing cycloidal mass analyzer, the peak width Δa is the same as the slit width. When ionizing a particle with a laser, the particle can act as a "virtual-slit" eliminating the need for a physical slit, and the peak with Δa at the detector is the size of the particle. There is also no need for an ion source as the particle can be ionized directly inside the mass analyzer. Furthermore, the virtual-slit enables a small instrument with high resolution, overcoming the throughput vs resolution trade-off when combined with the ability of the cycloidal mass analyzer to collect ions with wide energy and angular dispersions. For example, with a 10 µm diameter particle and 10 µm wide detector pixels, the configuration shown in Figure 4C has a resolution of 0.1 u, a resolving power of 3000 at m/q = 300 u, and requires an area of just 9 x 13 cm for the ion trajectories. Therefore, the unique focusing properties of the cycloidal mass analyzer enables collection of ions with the wide range of energy and angular dispersion generated by laser ionization without the need for additional focusing optics (Figure 3C) and enables using the size of the particle as a virtual-slit for high resolution in a small size.

6 Conclusion

In conclusion, cycloidal mass analyzers have unique perfect focusing properties not exhibited by any other mass analyzer. These properties include the ability to focus ions independent of their initial velocity as well as enabling a focal plane where ions are focused and detected. Despite these advantages, there have been relatively few examples of cycloidal mass analyzer use in the literature. This is due to the requirement of an array detector that functions in a magnetic field and detects low energy ions to take full advantage of the unique properties of the cycloidal mass analyzer. The recently developed CTIA array detectors provide a solution to these issues and enables several novel applications of the cycloidal mass analyzer including spatial aperture coding to increase throughput without sacrificing resolution and single particle mass analysis using the particle as a virtual-slit to enable high resolution in a small sized instrument.

7 Acknowledgements

The information, data, or work presented herein was funded in part by the Advanced Research Projects Agency-Energy (ARPA-E), U.S. Department of Energy, under Award Number DE- AR0000546 National Science Foundation under Award Number 1632069, National Aeronautics and Space Administration under Grant No. 80NSSC19K1027, by the Office of the Director of National Intelligence (ODNI), Intelligence Advanced Research Projects Activity (IARPA), via 2019-19031300004, and by the North Carolina Biotechnology Center via 2019-TEG-1502. The views and opinions of authors expressed herein do not necessarily state or reflect those of the United States Government or any agency thereof.

8 References

- 1. Bleakney, W.; Hipple, J. A., Jr., A new mass spectrometer with improved focusing properties. *Phys. Rev.* **1938**, *53* (7), 521-529.
- 2. Yates, R. C., A Handbook on Curves and Their Properties. J.W. Edwards: 1947.
- 3. Hites, R. A., Development of Gas Chromatographic Mass Spectrometry. *Anal. Chem.* **2016**, *88* (14), 6955-6961.

- 4. Blaser, W. W.; Bredeweg, R. A.; Harner, R. S.; LaPack, M. A.; Leugers, A.; Martin, D. P.; Pell, R. J.; Workman, J.; Wright, L. G., Process Analytical Chemistry. *Anal. Chem.* **1995**, *67* (12), 47-70.
- 5. Portable Analytical Instruments. *Anal. Chem.* **1991,** *63* (11), 641A-644A.
- 6. Blase, R. C.; Miller, G.; Westlake, J.; Brockwell, T.; Ostrom, N.; Ostrom, P. H.; Waite, J. H., A compact E × B filter: A multi-collector cycloidal focusing mass spectrometer. *Rev. Sci. Inst.* **2015**, *86* (10), 105105.
- 7. Amsden, J. J.; Herr, P. J.; Landry, D. M. W.; Kim, W.; Vyas, R.; Parker, C. B.; Kirley, M. P.; Keil, A. D.; Gilchrist, K. H.; Radauscher, E. J.; Hall, S. D.; Carlson, J. B.; Baldasaro, N.; Stokes, D.; Di Dona, S. T.; Russell, Z. E.; Grego, S.; Edwards, S. J.; Sperline, R. P.; Denton, M. B.; Stoner, B. R.; Gehm, M. E.; Glass, J. T., Proof of Concept Coded Aperture Miniature Mass Spectrometer Using a Cycloidal Sector Mass Analyzer, a Carbon Nanotube (CNT) Field Emission Electron Ionization Source, and an Array Detector. *J. Am. Soc. Mass Spectrom.* **2018**, *29* (2), 360-372.
- 8. Nier, A. O., A Mass Spectrometer for Routine Isotope Abundance Measurements. *Rev. Sci. Inst.* **1940**, *11* (7), 212-216.
- 9. Koppenaal, D. W.; Barinaga, C. J.; Denton, M. B.; Sperline, R. P.; Hieftje, G. M.; Schilling, G. D.; Andrade, F. J.; Barnes, J. H.; Iv, I. V., MS Detectors. *Anal. Chem.* **2005**, *77* (21), 418 A-427 A.
- 10. Hahn, Y. B.; Hebner, R. E.; Kastelein, D. R.; Nygaard, K. J., Channeltron Gain in Magnetic Fields. *Rev. Sci. Inst.* **1972**, *43* (4), 695-696.
- 11. Oba, K.; Rehak, P., Studies of High-Gain Micro-Channel Plate Photomultipliers. *IEEE Trans. Nucl. Sci.* **1981**, *28* (1), 683-688.
- 12. Smith, D.; Adams, N. G., An improved detector for a multicollector, cycloidal focusing, magnetic mass spectrometer. *J. Phys. E Sci. Instrum.* **1975**, *8* (1), 44.
- 13. Adams, N. G.; Smith, D., A multicollector, cycloidal focusing, magnetic mass spectrometer. *J. Phys. E Sci. Instrum.* **1974**, *7* (9), 759.
- 14. Peko, B. L.; Stephen, T. M., Absolute detection efficiencies of low energy H, H-, H+, H2+ and H3+ incident on a multichannel plate detector. *Nucl. Instrum. Methods Phys. Res. B* **2000**, *171* (4), 597-604.
- 15. Barnes; Sperline, R.; Denton, M. B.; Barinaga, C. J.; Koppenaal, D.; Young, E. T.; Hieftje, G. M., Characterization of a Focal Plane Camera Fitted to a Mattauch–Herzog Geometry Mass Spectrograph. 1. Use with a Glow-Discharge Source. *Anal. Chem.* **2002**, *74* (20), 5327-5332.
- 16. Knight, A. K.; Sperline, R. P.; Hieftje, G. M.; Young, E.; Barinaga, C. J.; Koppenaal, D. W.; Denton, M. B., The development of a micro-Faraday array for ion detection. *Int. J. Mass Spectrom.* **2002**, *215* (1–3), 131-139.
- 17. Schilling, G. D.; Andrade, F. J.; Barnes; Sperline, R. P.; Denton, M. B.; Barinaga, C. J.; Koppenaal, D. W.; Hieftje, G. M., Characterization of a Second-Generation Focal-Plane Camera Coupled to an Inductively Coupled Plasma Mattauch–Herzog Geometry Mass Spectrograph. *Anal. Chem.* **2006**, *78* (13), 4319-4325.
- 18. Schilling, G. D.; Ray, S. J.; Rubinshtein, A. A.; Felton, J. A.; Sperline, R. P.; Denton, M. B.; Barinaga, C. J.; Koppenaal, D. W.; Hieftje, G. M., Evaluation of a 512-Channel Faraday-Strip Array Detector Coupled to an Inductively Coupled Plasma Mattauch–Herzog Mass Spectrograph. *Anal. Chem.* **2009**, *81* (13), 5467-5473.
- 19. Schilling, G. D.; Shelley, J. T.; Barnes, J. H.; Sperline, R. P.; Denton, M. B.; Barinaga, C. J.; Koppenaal, D. W.; Hieftje, G. M., Detection of Positive and Negative Ions from a Flowing Atmospheric Pressure Afterglow Using a Mattauch-Herzog Mass Spectrograph Equipped with a

- Faraday-Strip Array Detector. *Journal of the American Society for Mass Spectrometry* **2010,** 21 (1), 97-103.
- 20. Felton, J. A.; Schilling, G. D.; Ray, S. J.; Sperline, R. P.; Denton, M. B.; Barinaga, C. J.; Koppenaal, D. W.; Hieftje, G. M., Evaluation of a fourth-generation focal plane camera for use in plasma-source mass spectrometry. *J. Anal. At. Spectrom.* **2011**, *26* (2), 300-304.
- 21. Scheidemann, A. A.; Ardelt, D.; Denton, M. B. APPARATUS FOR DETECTING PARTICLES 7,511,278, 2009.
- 22. Gresham, C. A.; Rodacy, P. J.; Denton, M. B.; Sperline, R. Micro faraday-element array detector for ion mobility spectroscopy. 6,809,313, 2004.
- 23. Gehm, M. E.; McCain, S. T.; Pitsianis, N. P.; Brady, D. J.; Potuluri, P.; Sullivan, M. E., Static two-dimensional aperture coding for multimodal, multiplex spectroscopy. *Appl. Opt.* **2006**, *45* (13), 2965-2974.
- 24. Eckhardt, C. J.; Gross, M. L., A proposed technique for signal multiplexing in mass spectrometry. *Int. J. Mass Spectrom. Ion Phys.* **1970,** *5* (3–4), 223-227.
- 25. Chen, E. X.; Russell, Z. E.; Amsden, J. J.; Wolter, S. D.; Danell, R. M.; Parker, C. B.; Stoner, B. R.; Gehm, M. E.; Glass, J. T.; Brady, D. J., Order of magnitude signal gain in magnetic sector mass spectrometry via aperture coding. *Journal of the American Society for Mass Spectrometry* **2015**, *26* (9), 1633-1640.
- 26. Russell, Z. E.; Chen, E. X.; Amsden, J. J.; Wolter, S. D.; Danell, R. M.; Parker, C. B.; Stoner, B. R.; Gehm, M. E.; Brady, D. J.; Glass, J. T., Two-dimensional aperture coding for magnetic sector mass spectrometry. *Journal of the American Society for Mass Spectrometry* **2015**, *26* (2), 248-256.
- 27. Amsden, J. J.; Gehm, M. E.; Russell, Z. E.; Chen, E. X.; Dona, S. T. D.; Wolter, S. D.; Danell, R. M.; Kibelka, G.; Parker, C. B.; Stoner, B. R.; Brady, D. J.; Glass, J. T., Coded apertures in mass spectrometry. *Annu. Rev. Anal. Chem.* **2017**, *10*, 141-156.
- 28. Chemistry WebBook, NIST standard reference database number 69. Linstrom, P. J.; Mallard, W. G., Eds. National Institute of Standards and Technology: Gaithersburg, MD, 2016.
- 29. Nash, D. G.; Baer, T.; Johnston, M. V., Aerosol mass spectrometry: An introductory review. *Int. J. Mass Spectrom.* **2006**, *258* (1–3), 2-12.
- 30. Murphy, D. M., The design of single particle laser mass spectrometers. *Mass Spectrom. Rev.* **2007**, *26* (2), 150-165.
- 31. Denoyer, E.; Van Grieken, R.; Adams, F.; Natusch, D. F. S., Laser microprobe mass spectrometry. 1. Basic principles and performance characteristics. *Anal. Chem.* **1982,** *54* (1), 26A-41A.
- 32. Bainbridge, K. T.; Jordan, E. B., Mass Spectrum Analysis 1. The Mass Spectrograph. 2. The Existence of Isobars of Adjacent Elements. *Phys. Rev.* **1936**, *50* (4), 282-296.
- 33. Mattauch, J.; Herzog, R., Über einen neuen Massenspektrographen. *Z. Physik* **1934**, *89* (11-12), 786-795.
- 34. Mamyrin, B. A.; Karataev, V. I.; Shmikk, D. V.; Zagulin, V. A., The mass-reflectron. A new nonmagnetic time-of-flight high resolution mass-spectrometer. *Zhurnal Ehksperimental'noj i Teoreticheskoj Fiziki* **1973**, *64* (1), 82-89.
- 35. Karataev, V. I.; Mamyrin, B. A.; Shmikk, D. V., New Method for Focusing Ion Bunches in Time-of-Flight Mass Spectrometers. *Sov. Phys.-Tech. Phys. (Engl. Transl.)* **1972,** *16* (7), 1177-9.
- 36. Sims, G. R., Principles of Charge-Transfer Devices. In *Charge-transfer devices in spectroscopy*, Denton, M. B.; Ratzlaff, K. L.; Sweedler, J. V., Eds. VCH: New York, 1994; pp 20-31.